Hindawi
International Journal of Antennas and Propagation
Volume 2023, Article ID 2038899, 19 pages
https://doi.org/10.1155/2023/2038899

*Research Article*

# Platform Tolerant RFID Tag Antenna Design for Safety and Real-Time Tracking of On-site Workers at Riskier Workplaces

**Aarti Bansal**,[1,2] **Rajesh Khanna**,[2] **and Surbhi Sharma**[2]

[1]*Department of Electronics and Communication Engineering, Chitkara University Institute of Engineering and Technology, Chitkara University, Rajpura, Punjab, India*
[2]*Department of Electronics and Communication Engineering, Thapar Institute of Engineering and Technology, Patiala, Punjab 147004, India*

Correspondence should be addressed to Aarti Bansal; aarti.bansal@chitkara.edu.in

Received 6 September 2022; Revised 21 November 2022; Accepted 25 March 2023; Published 21 April 2023

Academic Editor: Hervé Aubert



The safety of workers is significant when talking about large risky workplaces such as construction job sites. Therefore, we proposed a UHF-RFID tag antenna that can be used to identify various Job site equipments and also construction workers by tagging their wearable helmets. Here, the compact, low profile, and simple structured platform-tolerant RFID tag antenna is proposed and optimized for metal sheet and ABS-based safety helmets. Furthermore, WTMiddleware (Worker Tracking Middleware) using Javascript, CSS, and HTML has been implemented to demonstrate a real-time secured web-based remote access of workers to provide their actual on-site monitoring and tracking of construction equipment carried/operated by the workers for tracking solutions. First, the fabricated tag's performance was tested successfully in an outdoor scenario on various mountable materials such as wood, glass, plastic, and metal. The tag yielded a reasonable read range of 5.9 m on metallic sheet and 7.1 m on plastic with the highest read distance of 9.3 m on a glass sheet. Also, the measurement setup along with developed WTMiddleware was deployed in an actual workplace to demonstrate practical utility of the designed tag affixed on workers' safety helmets. It was observed that all the workers wearing tagged helmets were successfully identified, tracked, and monitored. Also, their real-time on-site details, working zone, and complete personal details were accessed through a developed web page application via WTMiddleware.

## 1. Introduction

In large job sites, constant supervision is required for site workers' safety besides taking care of different equipment used during construction. Additionally, managing effective access control in construction job sites poses a significant challenge in terms of the complexity of risky or construction site's layout [1, 2]. Therefore, it is necessary to monitor the workers and other staff for their safety concerns and effective site management. Hence, a traceability system is considered one of the necessary factors in tracking and tracing these workers and equipment at riskier workplaces.

Recently, Internet of Things (IoT)-enabled radio frequency identification (RFID) systems have been recently utilized in traceability systems, such as for food [3], material management [4], smart logistic applications [5], warehouse management [6], and many more. RFID, an auto-identification technology, is a key enabling technology for implementing an IoT network [7]. The data of the tagged object is stored in the RFID chip integrated with the tag. The reader captures this stored data, and the acquired information is further transferred to the cloud database for remote access and monitoring objects. Hence, RFID is not only being employed for identification but also for special applications, e.g., hydrogen concentration monitoring [8], structural health monitoring [9], screw relaxing monitoring [10], and human parameters monitoring [11]. This is possible due to its benefits of easy deployment and low-cost solutions [12–14]. IoT-enabled RFID systems are also pivotal for achieving accurate tracking and effective access control at construction sites. In [15], the author discussed the possibility of developing integrated smart OHS (occupational

health and safety) system design for construction sites by implementing monitoring-enabled wearable equipment and making them mandatory for the workers. But the implementation of a complete IoT-enabled RFID system with backend server connectivity for construction sites has never been reported in the literature.

The classic UHF-RFID system comprises a reader device equipped with reader antennas and tags. The material of the objects to which the tags are affixed significantly interferes with the RFID operation. Therefore, it is essential to evaluate the performance of RFID tags [16] under the influence of equipped object material. In developing a UHF-RFID system, tag antenna design faces a significant challenge due to interference from surrounding objects or environments [17]. The noises generated due to the multipath effect and signal interference deteriorates the backscattering process. Also, as the tag needs to be placed on different objects to be tracked, its radiation performance is strongly affected [18]. Due to the presence of conductive objects such as metal and liquid-containing objects, the incident signal is added destructively to the image current from these surfaces [19]. This results in degrading the performance of the tag antenna parameters such as input impedance, power transfer coefficient, radiation efficiency, and realized gain. More commonly, the passive tag must be mounted at a distance from the metal surface (around 1 cm), as stated in [20]. Also, there should be special considerations if some other nearby electromagnetic sources is working with the same operating frequency range. A more comprehensive study has been represented in [21], which discusses the interference of metal surfaces on passive tags. The author demonstrated that the tag antenna receives more power to wake up the chip when placed at $\lambda/4$ (being $\lambda$ the wavelength) distance from the surface. Different solutions are proposed in the recent literature to overcome these constraints for improving the performance of the tag antenna [22–25]. Recently, platform-tolerant tags have been designed to exhibit a higher read range in free space and when mounted on metal surfaces. There are commercial tags available that are mountable on metal. However, they are having larger dimensions with a bulky structure [26, 27].

Furthermore, a Middleware must be developed with RFID technology to implement the entire IoT-enabled UHF-RFID RFID traceability system. RFID middleware acts as an interface between the RFID hardware system and its application. Thus, middleware handles all the incoming real-time data from the connected reader without any read miss. Furthermore, it also serves to process the counting, filtering, and collecting of the tag data [28–32]. In [33], Haibi et al. developed a Middleware named BTMiddleware that uses MongoDB NoSQL database. This middleware was implemented for baggage traceability at airports, and the program was written in NetBeans IDE as the development environment using Java as the backend language. The user has the manual task of adding the reader name and IP address of the reader on the home page of the middleware to access the information. Remote access to the data recorded has been provided. Also, in [5], a Middleware combining block chain and RFID was designed to make the supply chain robust and secure. In this work, liquid bottles were tracked as they moved forward in the supply chain from the manufacturer to the retailer by attaching tags to them. The mobile application for remote access was implemented in a real-world scenario using block chain technology. It has a high accuracy varying between 92.5 and 97.5 percent. However, the time for mining each block varies due to the difference in input string lengths resulting in the variation of the transaction cost, which is the drawback of block chain. Extending the given concept for a risky construction site, we have designed an IoT-enabled UHF-RFID system by developing a worker tracking WTMiddleware. The proposed approach demonstrates a real-time secure web-based solution for workers' tracking, actual site monitoring, and tracking of vehicles/equipment. Following contributions are made in this study:

(i) The compact microstrip patch dipole configuration-based UHF-RFID tag antenna has been designed and optimized for mounting hard-to-tag metal-based equipment and the safety helmet.

(ii) The read range performance of the proposed RFID tag design has been experimentally validated on a metallic sheet and safety helmet using Impinj R420 reader and circularly polarized (CP) RFID reader antenna.

(iii) We designed WTMiddleware for enabling traceability and effective access control using a cloud-hosted NoSQL database. The developed middleware shows the potential to revolutionize effective management at the job site.

The robustness and feasibility of the proposed IoT-enabled UHF-RFID tracking system is demonstrated by experimental testing at a real job site scenario. The rest of the article is organized as follows: Section II, "IoT-Enabled UHF-RFID system architecture," introduces the analogous hardware-hardware configuration. After that, section III, "Integrated RFID system hardware with WTMiddleware," provides the relevant description of hardware and software development features. This section also provides guidelines regarding the design in the subsection titled "Tag Design and Analysis." The optimization of the tag antenna design for mounting it on a metal sheet and ABS plastic-based safety helmet is shown in the subsection titled "Parametric Study of proposed dipole tag."

Furthermore, the impedance characterization, read range measurements, and their validation for the fabricated prototype of the designed tag is presented. The software implementation and hardware management interface details are given under the subsection "WTMiddleware Design." Furthermore, the details of on-site testing of the complete system are outlined under the "Real-time testing" section. Finally, the significant contributions of this research study are discussed under the "Conclusions" section.

## 2. IoT Enabled UHF-RFID System Architecture

The system model to attain total digital worksite visibility of workers using the IoT-enabled RFID system is illustrated in Figure 1. The proposed scheme provides real-time

application for tracking and providing access control at the job site. The proposed framework has the following significant blocks:

*2.1. Personnel/Equipment Reading Block.* The reader transmits a continuous wave (CW) signal for a specific duration (predefined) with maximum power to charge all the tags under its coverage range. Thus, in the personnel/equipment reading block, the data related to worker/equipment (hauling/lifting) will be read from the RFID affixed gadget and registered in the database.

*2.2. Data Acquisition Block.* In the data acquisition block, the tagged gadget/equipment data will be read by deployed UHF reader and fed to the WTMiddleware. Here, the reader identifies the tagged workers falling in the range of the reader.

*2.3. WTMiddleware Block.* In the WTMiddleware block, acquired data is further processed, translated, and authenticated using a web-based application for remote access by the supervisor. Here, an onsite monitoring operation is performed to verify workers present at the job site. If any worker is not present or the tag is not replying, it will inform the monitoring computer to raise the alarm to notify the supervisor. A detailed explanation of the integrated hardware-Middleware is given in the next section.

## 3. Integrated RFID System Hardware with WTMiddleware

RFID system hardware consists of an RFID reader connected to the reader antenna, RFID tag, and host computer. For the WTMiddleware design, CSS and HTML have been used to design the webpage frontend; NoSQL and Javascript have been used as backend language. The typical view of the integration of RFID system hardware with WTMiddleware is shown in Figure 2. A detailed discussion of hardware and WTMiddleware is given below.

### 3.1. RFID System Hardware

*3.1.1. RFID Reader.* In the proposed system, we used a 4-port Impinj R420 reader with 32-read zones to support different locations around the working or job site area in a complex construction site. The deployed reader has a receiver sensitivity of −84 dBm with a maximum transmit power of 32.5 dBm. The reader is connected to a circularly polarized broadband (860–940 MHz) reader antenna. The reader interrogates the tagged objects by sending the modulated signal towards the tag. The reader receives the backscattered signal from the tag containing the required information. The installed reader will automatically receive the data transmitted by the tag-equipped gadgets from different locations.

*3.1.2. RFID Tag.* The details of each worker, including their entry/exit time and location, are stored in the RFID tag mounted on the safety helmet. The function of the tag is to transmit the worker's unique identity (ID) number to the allocated RFID reader. Thus, each worker under the specific reading zone is continuously scanned and monitored in real-time. Additionally, tracking metal-based equipment will efficiently manage the overall construction site. This will also prevent mishandling of harmful equipment.

*(1) Tag Design and Analysis.* As already discussed, the tag performance gets detuned when tagged on different objects such as metal and objects with different dielectric properties (liquid-containing bottles, plastic, wood, glass, etc.). Therefore, the codesign approach was implemented, considering the effect of the metallic object and ABS-based helmets, respectively. Here, a microstrip patch-based dipole tag antenna is designed to work in the ETSI band (865–867 MHz) to provide a low-cost, platform-tolerant, and most optimal solution. The proposed UHF-RFID tag and codesign model (on metal and safety helmet) are shown in Figures 3 and 4, respectively. The proposed tag comprises a two-layered structure with the top layer as a radiating dipole and the bottom layer as a metallic ground.

Two shorting pins/vias are employed at its edges to connect the top patch layer and the ground plane for the design purpose. The Alien Higgs-3 RFID chip [34] is assumed to be integrated into the middle of the dipole arms of the antenna configuration. The impedance of the employed Higgs-3 chip was obtained considering its parameters $C_{ic} = 0.85$ pF and $R_{ic} = 1.5\,k\Omega$ provided in the datasheet [34] with an equivalent impedance value of $27\text{-}j\,212\,j$ at 866 MHz. This forms a "3D inductive loop" to exhibit high inductive reactance to compensate for the capacitance of the RFID chip. The tag is optimized by placing it on the metal sheet and ABS-based plastic safety helmets.

*(2) Parametric Studies of Proposed Dipole Tag.* The rigorous analysis of the designed tag antenna on the metal sheet (200 mm × 200 mm) was conducted by performing its parametric study based on its geometrical dimension variations. Figures 5(a) and 5(b) show that the real and imaginary component of the tag's impedance decreases as the length of the upper slot, i.e., "$L_1$" increases (varied from 4 mm to 6 mm in steps of 0.5 mm). Also, the gain of the tag antenna increases with increasing "$L_1$" under the influence of the back object, as observed from Figure 6. Hence, the optimum value of slot length, "$L_1$" = 5 mm, was chosen to trade-off between both conjugate impedance and gain.

Furthermore, Figures 7(a) and 7(b) show the variations in the real and imaginary components of tag impedance with respect to variation in space between the dipole arms, i.e., "$w_1$" from 3.5 to 4.5 mm (in steps of 0.5 mm), respectively. There is a slight increase in the values of both impedance components, i.e., resistance and inductance, with respect to the increase in "$w_1$." Also, from Figure 8, the gain of the designed tag increases with an increase in the center space between the dipole arms. This is justified because the field in the opposite dipole gets canceled as the distance "$w_1$" decreases. This further leads to reduced gain. Therefore, the space between the dipole arms is optimized to achieve conjugate impedance matching and gain. The optimum value of "$w_1$" is selected to be 4.5 mm.

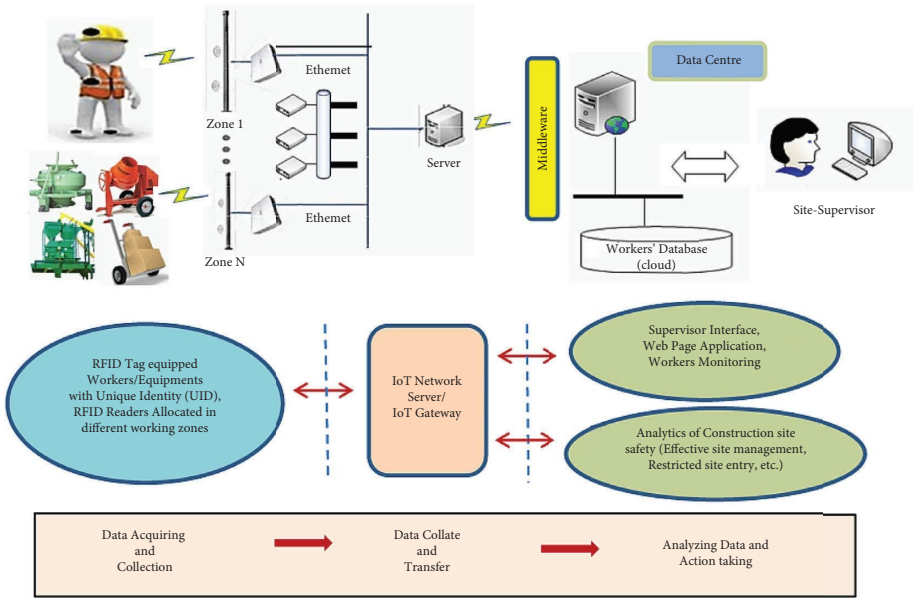


Figure 1: IoT-enabled UHF-RFID system architecture.

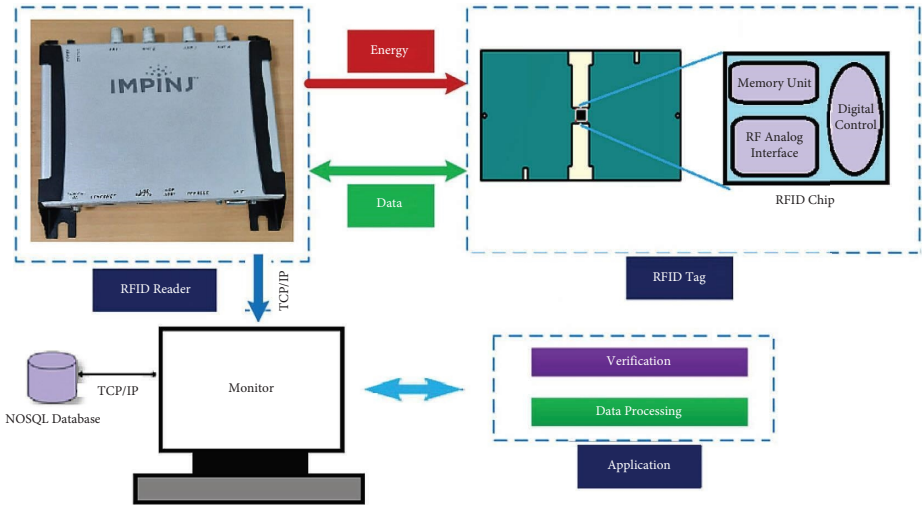


Figure 2: Integrated RFID system hardware with WTMiddleware.

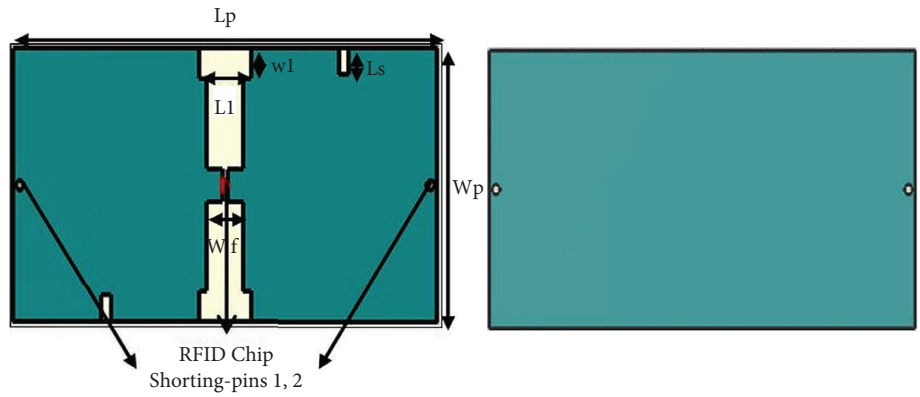


Figure 3: Patch based dipole tag antenna configuration.

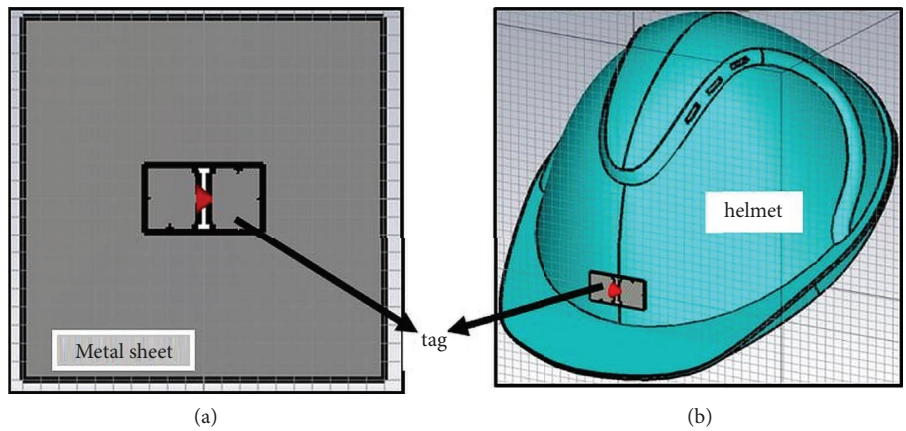


Figure 4: Tag Codesign on (a) metallic surface and (b) ABS plastic-based safety helmet.

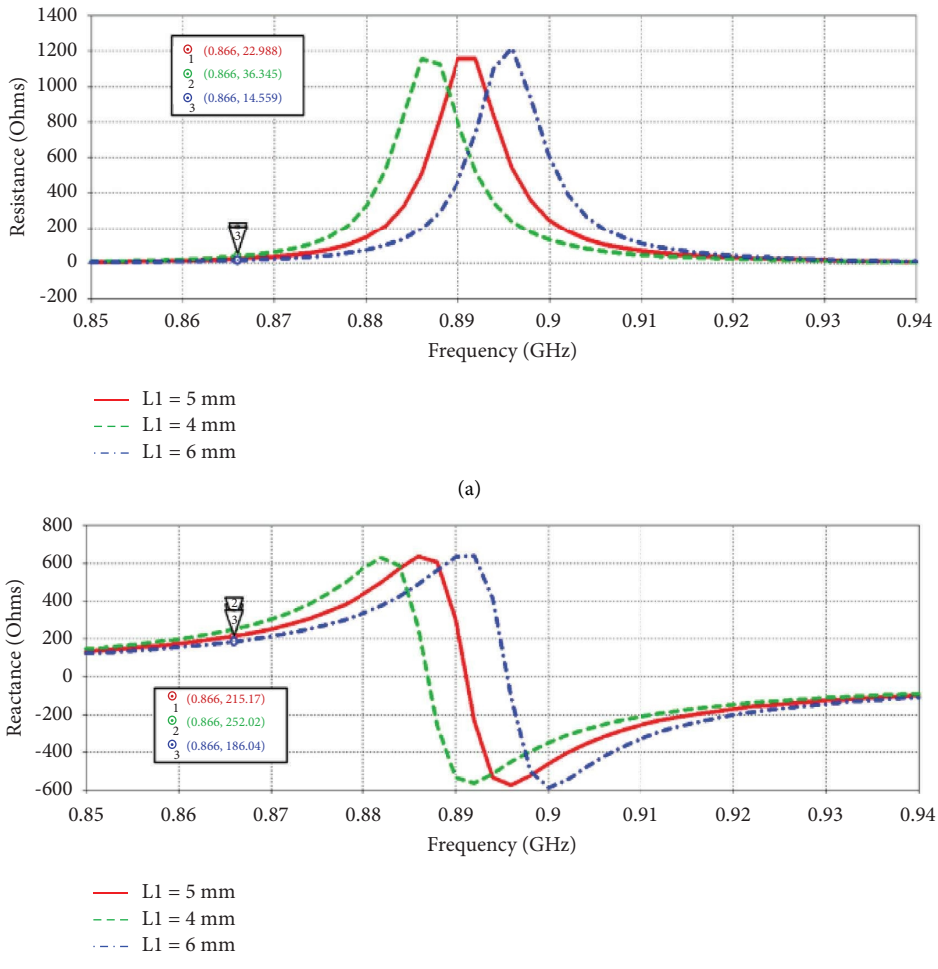


Figure 5: Tag's (a) resistance and (b) reactance variation with "$L_1$."

Moreover, the effect of change in the "$w_f$" (feed width) parameter on the tag's impedance is shown in Figure 9. It is observed that both real and imaginary components of the tag impedance rise significantly with the increase in value of "$w_f$" (varied from 2.48 to 3.48 mm in steps of 0.5 mm). Also, Figure 10 indicates that the gain of the designed tag antenna increases with an increase in value of "$w_f$." The optimum value chosen for "$w_f$" is determined to be 2.98 mm.

Here, the variation in its impedance and gain is studied by varying the size of the metal sheet (200 mm × 200 mm, 300 mm × 300 mm, and 400 mm × 400 mm). It is observed that the impedance of the designed tag remains stable with

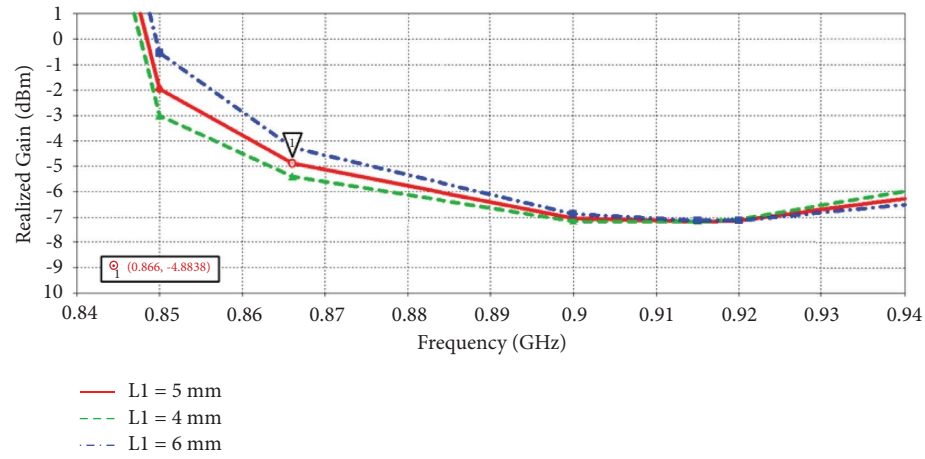


Figure 6: Gain performance of the tag with varying "$L_1$."

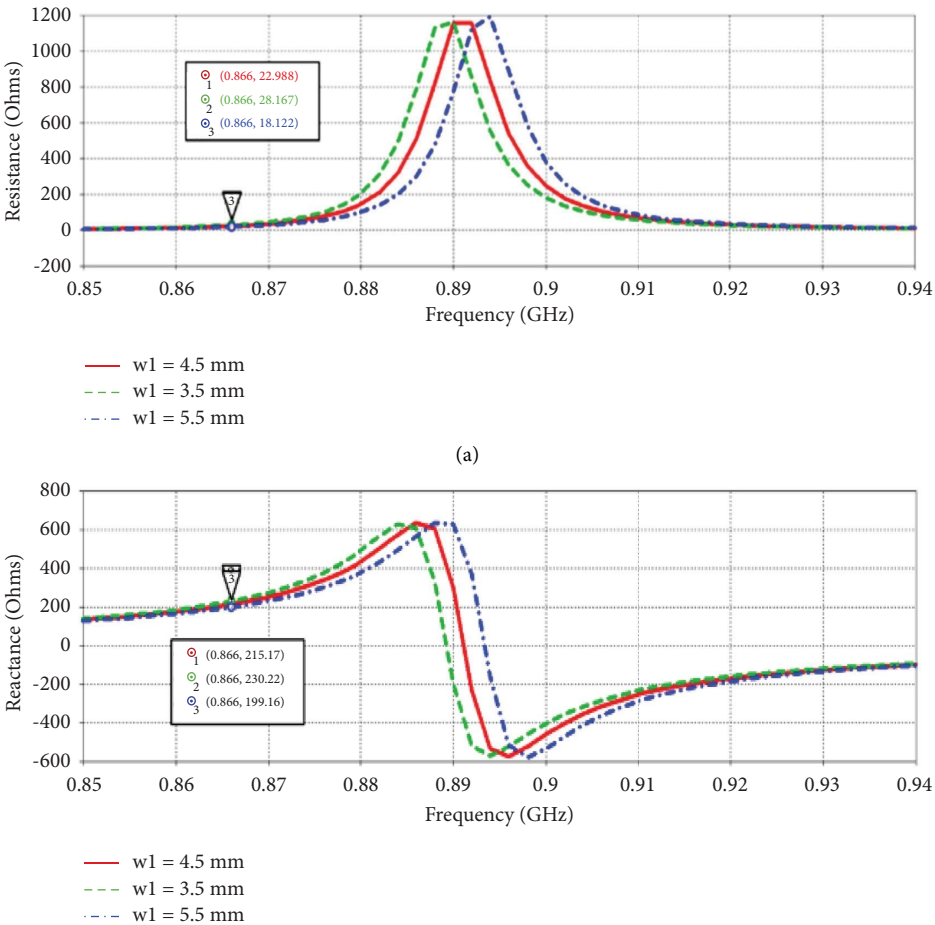


Figure 7: Tag's (a) resistance and (b) reactance variation with varying "$w_1$".

the increase in the size of the metal sheet (Figure 11), validating its platform tolerance capability. However, from Figure 12, the gain of the tag is observed to decrease as the metal sheet size increases.

The designed tag antenna was simulated and designed using CST software version 2018. Table 1 shows the optimized dimensions of the designed tag antenna for mounting on both platforms, i.e., metal sheet and safety helmet.

The simulated tag antenna was fabricated by etching 0.035 mm copper on a RO 4350 B substrate (permittivity of 3.3 and loss tangent of 0.0031), as shown in Figure 13.

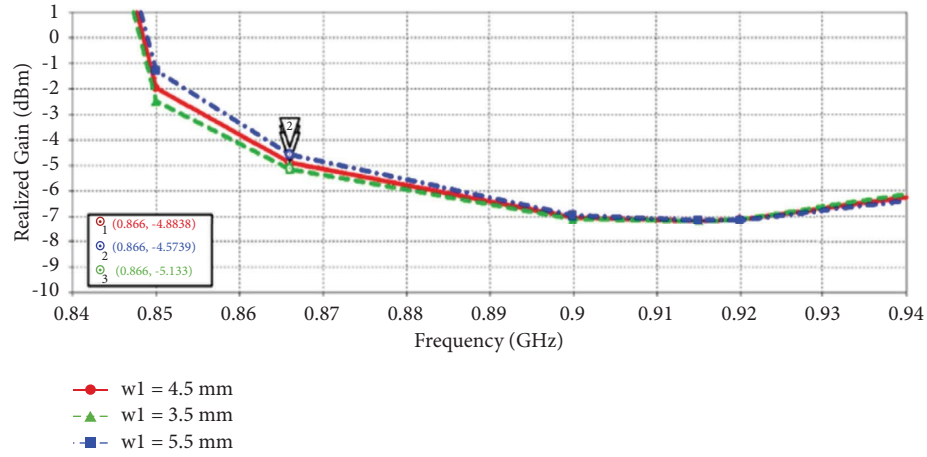


FIGURE 8: Gain performance of the tag with varying "$w_1$".

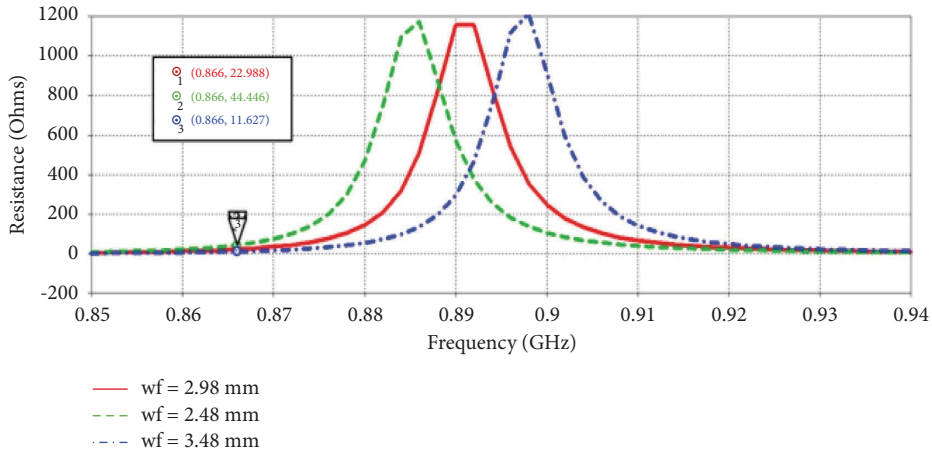


(a)

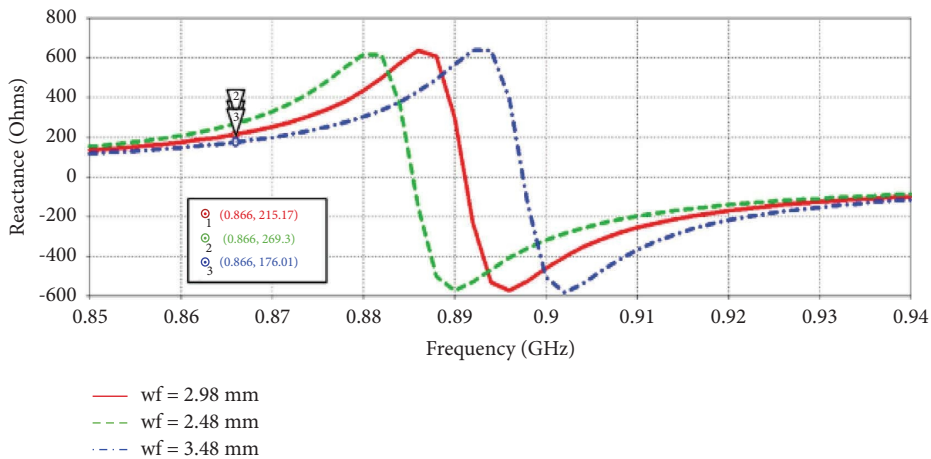


(b)

FIGURE 9: Tag's (a) resistance and (b) reactance variation with varying "$w_f$".

For analyzing the fabricated prototype performance for practical utility, impedance measurement and read range testing was performed. The impedance of the tag was measured by employing the tag inlay without an RFID chip, as shown in Figure 14(a). The impedance of the designed tag was measured using a differential probe set up and vector network analyzer E5071C following port extension calibration as detailed in [35]. The input impedance of the proposed tag antenna, $Z_{in}$ was calculated using the following equation:

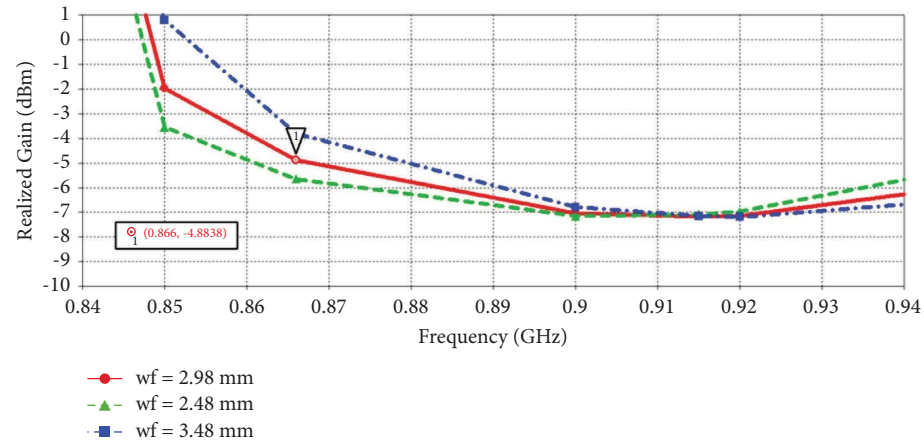


FIGURE 10: Gain performance of the tag with varying "$w_f$".

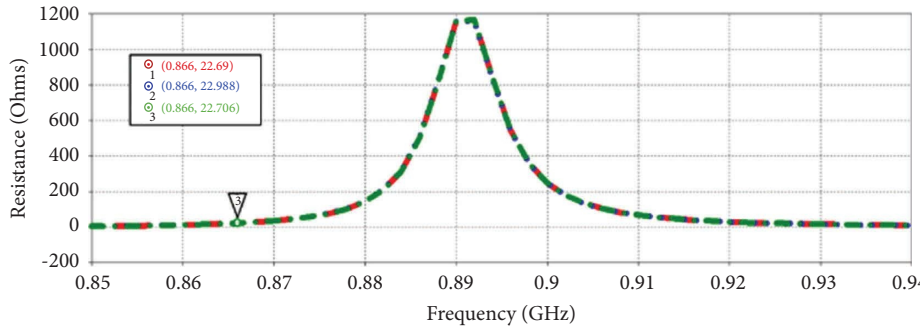


(a)

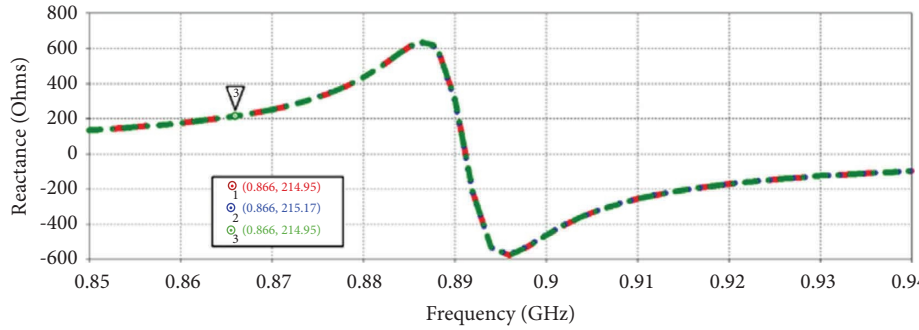


(b)

FIGURE 11: Tag's (a) resistance and (b) reactance variation with varying metal sheet size.

$$Z_{in} = \frac{2\,Z_0\left(1 - S_{11}S_{22} + S_{12}S_{21} - S_{12} - S_{21}\right)}{\left(1 - S_{11}\right)\left(1 - S_{22}\right) - S_{21}S_{12}}, \quad (1)$$

where $Z_0$ is the characteristic impedance of coaxial lines. The helmet's material was chosen to be ABS plastic having a relative permittivity, $\varepsilon r = 3.5$. Furthermore, the employed Higgs-3 chip impedance simulated and measured tag antenna's impedance after mounting on a metal sheet (with dimensions $200 \times 200\,\text{mm}^2$) are plotted in Figure 14(b), respectively. It is observed that the measured impedance of the tag is $26.3 + j\,222.2$ Ohms compared to the simulated tag antenna's impedance of $22.9 + j\,215.1$ Ohms at a resonant frequency of 866 MHz, validating a good impedance match in the ETSI RFID band, respectively. The slight difference in

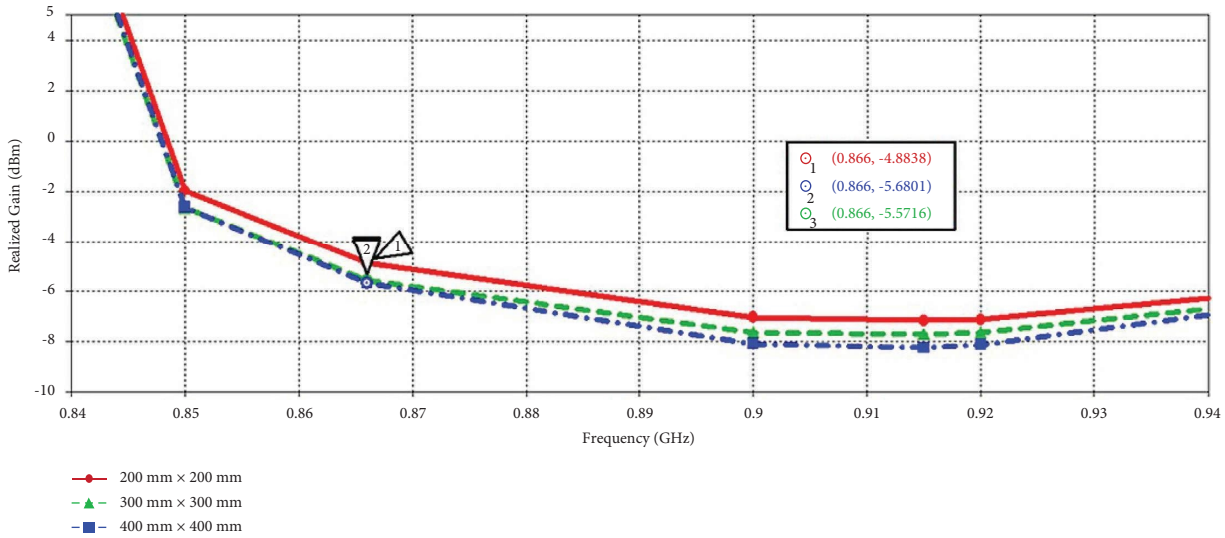


Figure 12: Gain performance of the tag with varying metal sheet size.

Table 1: Optimized dimensions of the proposed tag.

| Parameter | On metal (mm) Dimension | On plastic helmet (mm) Dimension |
|---|---|---|
| $L_p$ | 65.2 | 65.2 |
| $W_p$ | 37 | 35 |
| $L_1$ | 10 | 10 |
| $W_1$ | 4.5 | 4.5 |
| $L_f$ | 4.34 | 3.59 |
| $W_f$ | 2.98 | 2.795 |
| $L_s$ | 3 | 3 |
| $W_s$ | 1.5 | 1.5 |
| $H_s$ | 0.8 | 0.8 |
| Via_radius | 0.65 | 0.65 |

the measured impedance compared to simulated impedance may be attributed to the fabrication tolerances and changes in the chip impedance. Also, there are accuracy issues concerned with using a differential probe setup for the impedance measurements method of the tag antenna. Furthermore, Figure 15 depicts the $S_{11}$ results to validate the impedance matching between the proposed tag antenna and microchip. It is observed that the measurement results agree well with the simulated $S_{11}$ results.

Furthermore, the $RF_1$ and $RF_2$ terminals of the Higgs-3 RFID microchip were soldered to the feeding port terminals of the designed tag antenna to measure its read range and its platform tolerance capability. The proposed tag's performance was verified by performing the read range measurement method using the Impinj R420 reader setup [36]. The experimental setup consists of an RFID reader connected to a circularly polarized reader antenna (gain of 9 dBi) and a host computer with an installed Impinj item test software setup. The measurement setup works by transmitting a reader input signal towards the tag-mounted helmet. The tag intercepts the part of this incident signal as there is a power loss accompanied in the free space and the cables of the setup. The RFID chip gets activated by utilizing this intercepted received power, and finally, the tag sends back the backscattered signal towards the reader setup. The host computer finally obtains this backscattered signal and receives data.

The read range performance of the proposed tag is validated in a real outdoor scenario by pasting the prototyped tag on metal and on the helmet and different dielectric surfaces (foam, plastic, wood, and glass), as depicted in Figures 16(a) and 16(b).

The read range was measured by moving the tag away from the reader and determining the maximum distance it could be recognized. Although the proposed tag was designed, simulated, and optimized to mount on metal equipment and wearable helmet, it was observed that it exhibited satisfactory performance on other objects (plastic, wood, foam, and glass) with different dielectric properties. Figure 17 shows the read range performance of the tag on different mounted objects.

The tag exhibited a read range of 5.9 m when pasted on the metal sheet ($200 \times 200\ mm^2$) and 7.1 m when mounted on an ABS plastic-based safety helmet. Also, the designed tag antenna exhibited a read range of 7 m, 4.9 m, 6.1 m, and 9.3 m when mounted on different material objects such as the plastic sheet, foam, wood, and glass, respectively, validating the designed tag's robustness.

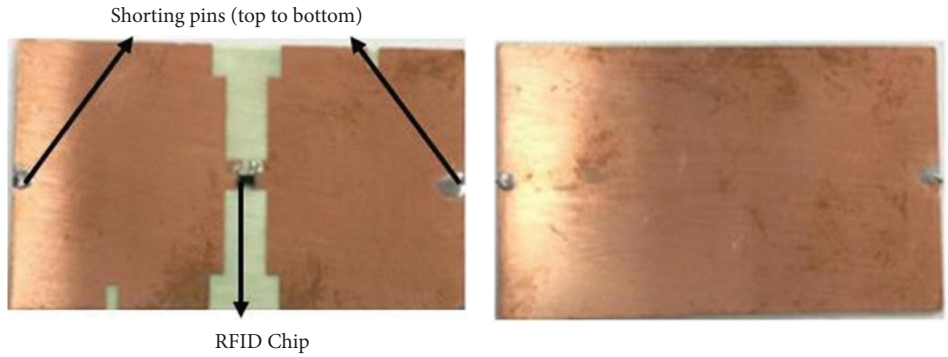


Figure 13: (a) Top and (b) bottom side of fabricated prototype of designed tag.

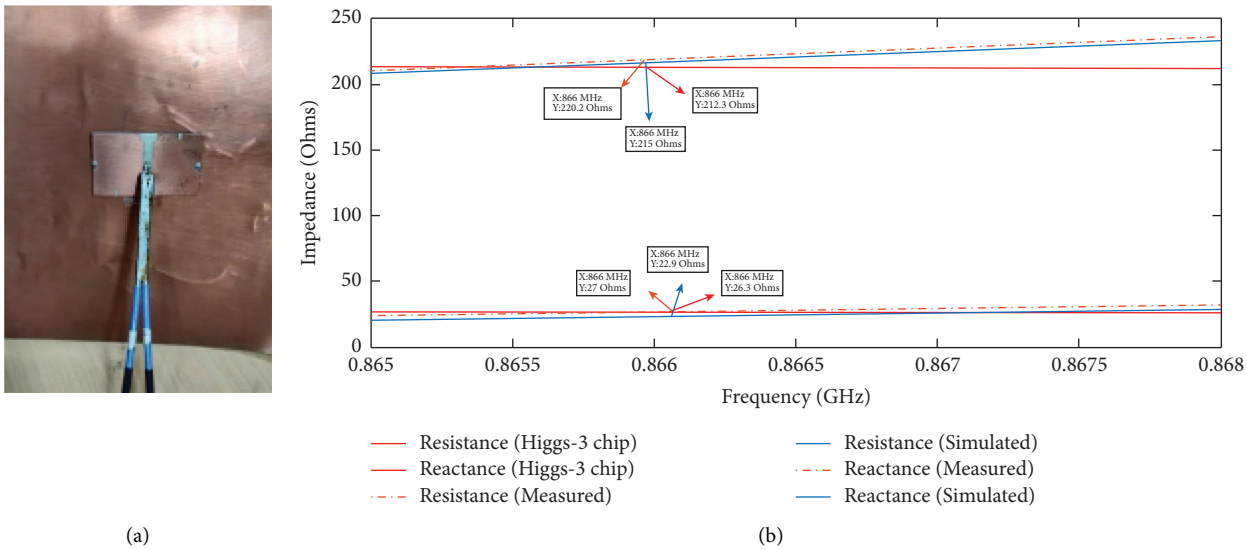


Figure 14: Simulated and measured impedance characteristics of the proposed tag (shown on left) on a metal sheet ($200 \times 200\,\text{mm}^2$).

Figure 18 shows the 3D radiation pattern of the tag at a center frequency of 866 MHz on the metal sheet and safety helmet. It is depicted that the tag pasted on the metal sheet exhibited a directional pattern with a gain of −4.88 dB on the metal sheet ($200 \times 200\,\text{mm}^2$) and −2.1 dB on the helmet (circumference of 10 cm) directivity of 4.15 dBi, demonstrating platform tolerance capability.

The comparison of the proposed tag's performance with respect to other recently developed tags has been carried out in Table 2.

The proposed tag is observed to exhibit a longer read range than that of tags designed in [37–45]. In addition, the size of the proposed tag is smaller than the designed tags in [37, 41, 43–47]. On the other hand, the tag's read range in [40, 47] is higher but with a larger size. In addition, the gain of the proposed tag is more as compared to tags designed in [37, 38, 43, 47], resulting in a higher read range. Furthermore, the tag designed in [46] needs to be placed at a gap of 0.2 mm from the conductive surface. Thus, the proposed tag is found to be potential candidate suitable for mounting on metal, plastic, wood, foam, and glass objects. Also, it has better performance in terms of size, gain, and read range, which is essential for tagging different jobsite equipment and worker's wearable helmet for tracking and access control. Furthermore, to interrogate the developed RFID prototype from a remote location, a suitable WTMiddleware has been designed for anywhere everywhere access of workers and tagged equipments.

*3.1.3. WTMiddleware.* The designed tag allocates a unique identity to the workers or equipment, which is necessary to monitor workers in real-time. The web application was deployed to enable tracking of workers by developing a WTMiddleware. In this middleware, a web-based application program is written to display the on-site working details of the workers performing the following main functions:

(i) Hiding all the information fetched by the hardware from the backend applications.

(ii) Removing all unwanted information that is not required to be shown to the end-user.

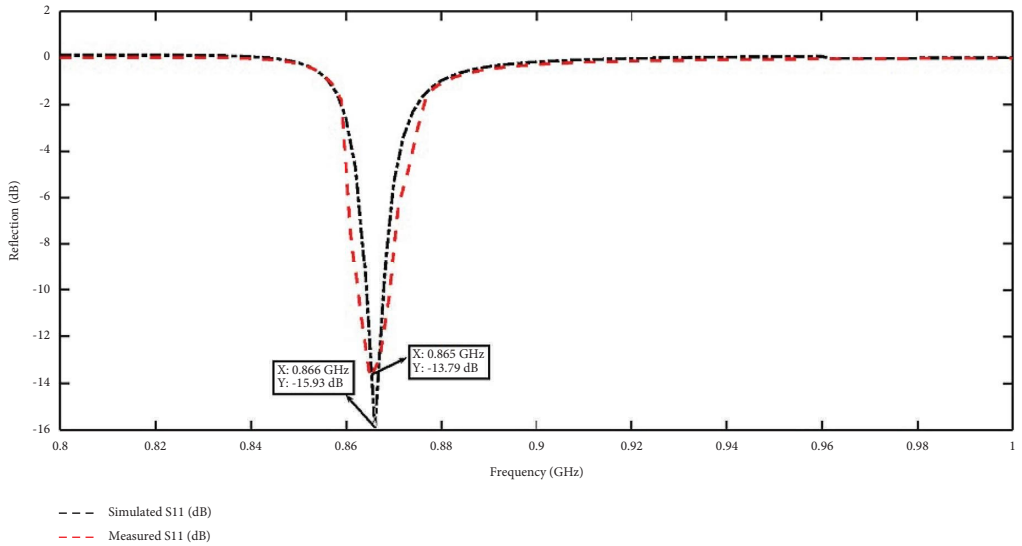


Figure 15: Simulated $S_{11}$ (dB) performance of the proposed tag.

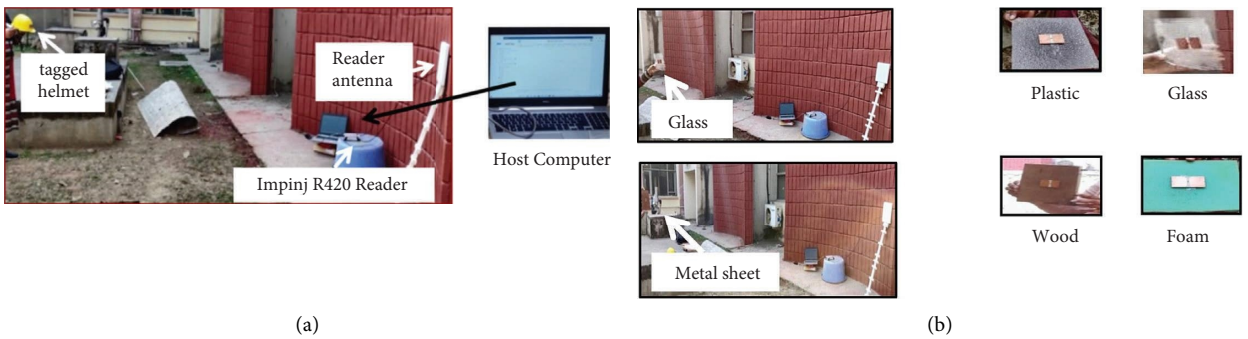


Figure 16: (a) Measurement set up (Impinj R 420 reader) to measure the read range performance of the designed tag in outdoor scenario. (b) Different material objects (metal-sheet, plastic, wood, and glass) on which tag is mounted.

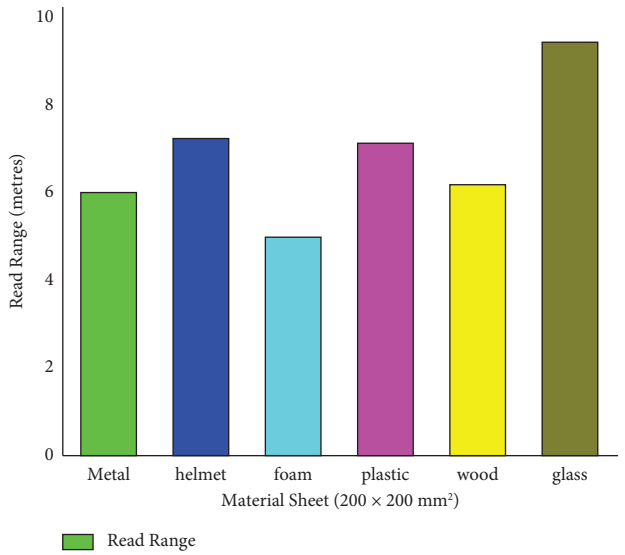


Figure 17: Read range of designed mounted on the metal sheet, ABS-plastic helmet, foam, wood, and glass objects.

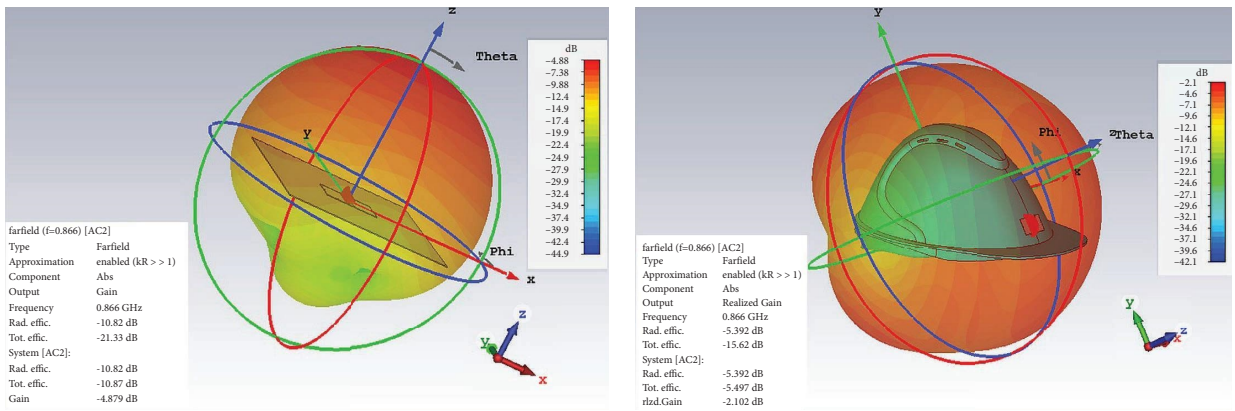


(a) (b)

Figure 18: 3D radiation patterns for the designed tag on the (a) metal sheet and (b) helmet.

(iii) Processing the raw data before using and sending it to other applications. It thus provides selectivity in choosing the readers and using information from different readers separately.

Figure 19 shows the WTMiddleware management interface presenting the communication between the reader and a web-based application. Here, CSS and HTML language were used to develop frontend web page design. The backend code for the developed middleware was performed using Javascript.

Reader interface provides an API to integrate data acquired through reader's item sense software into the website. The readers are connected through Wi-Fi/Ethernet connection to communicate with the installed servers. Furthermore, the middleware management layer also provides link to the database storage using the NoSQL cloud Firebase [28].

In the WTMiddleware design, Algorithm 1 illustrates the authentication of the supervisor to prevent data theft and verify only authorized personnel to access this information.

If the email id and password match the one stored at the backend, the user is taken to a select page with three options: worker details, current on-site details, and logout. The worker details page will have the stored data such as name, address, and contact details and verify the authorized workers from the firebase database. The current on-site details are the page for monitoring on-site worker's status and location. Finally, the logout page will direct the user to the login page. Figure 20 shows "Login Interface for Supervisor Login and Start-up Interface," in which the login will be provided to the supervisor through the login interface for authentication purposes.

The authenticated supervisor is required to enter an email id and password for login. In the start-up interface, the webpage will direct the supervisor to observe the information regarding the authorized workers (EPC ID, name, address, and contact) and their real-time onsite details. The pseudocode of Algorithm 1 and the developed page using the algorithm is given as follows:

Algorithm 2 demonstrates the process of implementation of on-site worker details. The onsite worker details are updated during each cycle of the data fetch process.

The variables such as worker's name, unique EPC product code, and timestamp show the present worker's status at the construction site. Initially, the data were received from the Impinj software in the form of a CSV file which is fetched every 5 seconds to keep the database updated. As the tag is read in every time step, the multiple EPC entries are merged to remove the duplicate entry in reading. At the end of each shift, the workers' EPC and total time fetched will be used as their on-site working time to calculate their daily wages. Also, the supervisor will have an automatic update of the shift ending time of each worker. Finally, the updated data will be automatically submitted to the firebase database. Figure 21 shows the developed web page for workers' personal details and the history of the authorized workers, which are stored in the firebase database record.

This web page will provide complete personal details such as the worker's name, address, and contact details. The supervisor can also access the details of the worker by inputting his unique EPC code. Thus, this cloud-based firebase app provides the security and authenticity for the real-time monitoring of workers.

The current on-site details page is shown in Figure 22. The page will display different data fields such as the timestamp, EPC product code, workers' location according to different reader antennas deployed in different working zones, and their calculated working hours. The timestamp shows the date and time when the worker enters the location. Other functionalities such as access control and alarm integration may be added further to restrict workers from entering dangerous zones.

## 4. Real-Time Testing of IoT-Enabled UHF-RFID System

For real-time testing and to validate application usage, the developed "IoT-Enabled UHF-RFID system" was tested at the construction site of B-block, Thapar Institute of

Table 2: Comparison of proposed tag with other tag.

| Reference | Tag antenna structure | RFID IC | Chip sensitivity (dBm) | EIRP (W) | Volumetric size ($L \times W \times H$) ($mm^3$) | Gain/directivity (dB/dBi) | Maximum read range on metal (meters) |
|---|---|---|---|---|---|---|---|
| [37] | Dual antenna patch structure | NXP's UCODE 7 | −21 | 3.3 | 10,264 | −4.98 dB | 4.3 m |
| [38] | Loop bowtie strap feed structure | Higgs-3 | −18 | 4 | 880 | −9 dB | 2.7 m |
| [39] | Dual loop structure | Higgs-3 | −18 | 4 | 742.5 | NA | 6.1 |
| [40] | Z-slot patch structure | Higgs-3 | −18 | 4 | 1140 | NA | 10 |
| [41] | Folded patch structure | Monza R6 | −20 | 3.28 | 2560 | NA | 5 |
| [42] | Single-layer meandered structure | SOT1040-1 chip | — | 1 | 1360 | 1.88 dBi | 5.78 m |
| [43] | Single-sided dual antenna structure | Monza 2 | −18 | 3.3 | 7840 | −9 dB | 6.0 m |
| [44] | Single-sided dual antenna structure | — | — | 4 | 5360 | 0 dBi | 4.4 m |
| [45] | Double-layer antenna with a rectangular loop | — | — | 4 | 2329 | — | 4 m |
| [46] | 3D-dipole antenna | Alien Higgs-4 chip | | 4 | 2800 | — | 5.1 m |
| [47] | Single-layer *U*-shaped feeder structure | Higgs-4 | −20.5 | 4 | 1950 | −8 dB | 6.9 |
| This work | Dipole 3D patch structure | Higgs-3 | −18 | 3.28 | 1872 | −4.87 dB/−2.1 dB metal/ helmet | 5.9 m/7.1 m metal/ helmet |

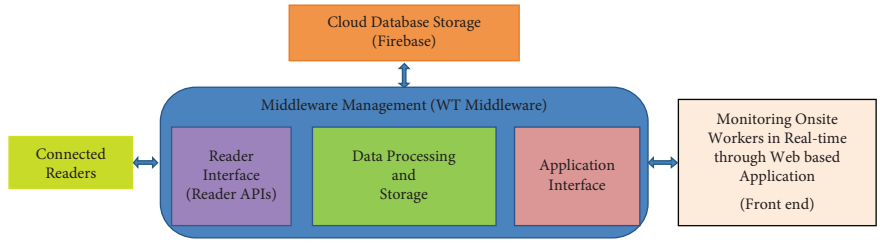


Figure 19: WTMiddleware management interface.

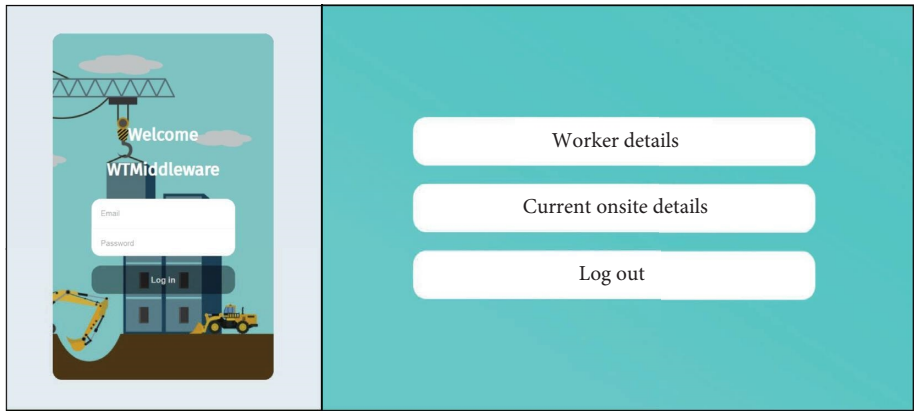


Figure 20: Login interface for supervisor and start-up interface.

```
(1) enter email and password
(2) if (email and password match) then
(3)       go to Select page
(4)       if (selected = worker details) then
(5)             go to page third1
(6)       else if (selected = current on-site details) then
(7)             go to page third2
(8)       else if (selected = logout) then
(9)             go to page index
(10)      End
(11) else
(12)      nvalid id or password
(13)      stay on index page
(14) End
```

Algorithm 1: Multiple page layout.

Engineering & Technology, Patiala. The workers' location and time information has been fetched and stored in the cloud-based firebase database through the designed middleware. For this, the designed tags were pasted over the helmet of the construction workers to monitor them, as shown in Figure 23. Furthermore, the complete measurement setup (zoomed) deployed at the real-time construction site for tracing the workers is shown in Figures 24(a)–24(c). The reader antenna was installed in the working zone to read the tagged workers' status in the testing setup. However, in the practical setup, multiple antennas may be deployed to cover the entire working area or multiple working zones so that the tags do not get blocked by the reader signal and go unidentified.

Figure 25(a) shows the tracked record of the workers on the item test software, and Figure 25(b) shows the real-time on-site workers' status displayed on the developed web application. The experiment was repeated three times, and it was observed that all of the workers were accurately tracked and monitored correctly. Furthermore, Figures 26(a)–26(c) showed the on-site details of the remaining workers when few of them left the construction site. Thus, the experiment showed good accuracy for the monitoring and tracking of workers, showing the designed system's robustness. Hence,

```
(1) btnsubmit < - SubmitButton
(2) csv < - comma separated values
(3) ts < - timestamp
(4) fetch csv file every 5 seconds
(5) split the received data into rows
(6) create an array of rows
(7) remove the first two entries of array displaying ts and reader details (not required in table)
(8) join the array back into rows
(9) get each cell entry separately using Papa.parse() function
(10) if (EPC is repeated) then
(11)       remove duplicate entry
(12)       else
(13)       add entry to table
(14) end
(15) add a column for time using add DataToTable()
(16) if (EPC read) then
(17)       start function showtime()
(18)       show time in the format 00: 00: 00
(19)          else
(20)          Return to step 9
(21) End
(22) if (time is equal to shift ending time) then
(23)          click btnsubmit automatically (visibility: hidden)
(24)          data is submitted
(25)          reset table
(26)          data stored in firebase backend
(27)          else
(28)          keep receiving data
(29) End
```

Algorithm 2:On-site worker details.

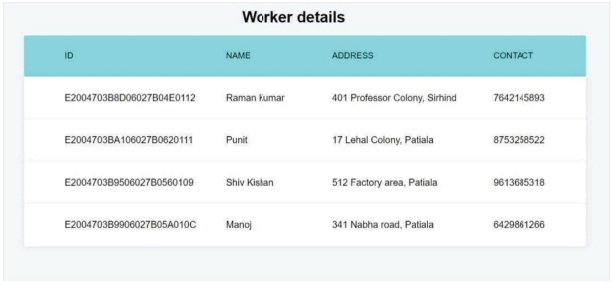


Figure 21: Worker's details through cloud database.

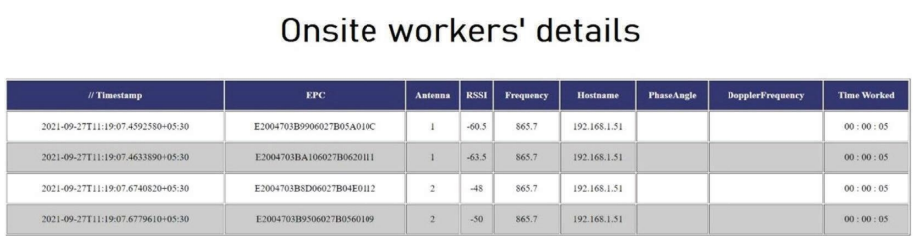


Figure 22: On-site details displayed on developed web application.

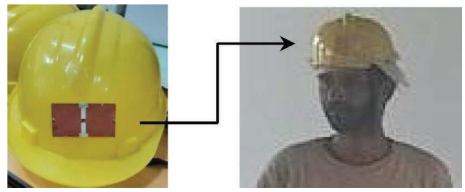

Figure 23: Tagged safety helmet mounted on construction worker.

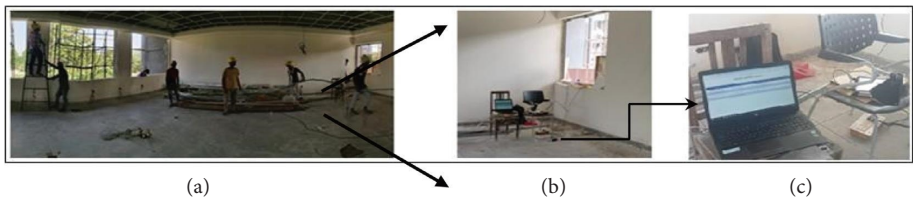

(a) (b) (c)

Figure 24: (a) Construction Site with multiple workers wearing tagged helmets. (b) On-site measurement setup. (c) Zoomed view of measurement set up.

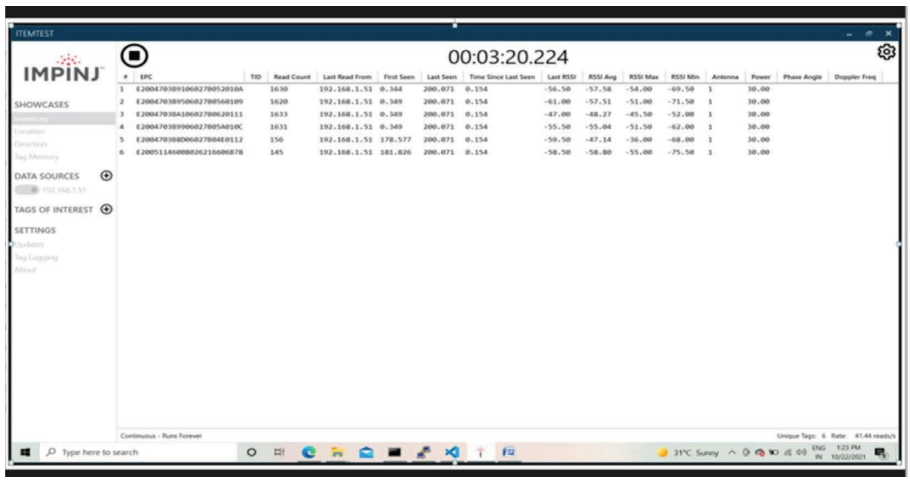


(a)

Onsite Working Details

| // Timestamp | EPC | Antenna | RSSI | Frequency | Hostname | Time Worked |
|---|---|---|---|---|---|---|
| 2021-10-22T00:52:34.5569820-07:00 | E2004703B9106027B052010A | 1 | -57.5 | 865.7 | 192.168.1.51 | 00 : 01 : 32 |
| 2021-10-22T00:52:34.5599240-07:00 | E2004703B9506027B0560109 | 1 | -56.5 | 865.7 | 192.168.1.51 | 00 : 01 : 32 |
| 2021-10-22T00:52:34.5632030-07:00 | E2004703BA106027B0620111 | 1 | -48.5 | 865.7 | 192.168.1.51 | 00 : 01 : 32 |
| 2021-10-22T00:52:34.5642470-07:00 | E2004703B9906027B05A010C | 1 | -55 | 865.7 | 192.168.1.51 | 00 : 01 : 32 |
| 2021-10-22T00:55:32.7354550-07:00 | E2004703B8D06027B04E0112 | 1 | -67.5 | 865.7 | 192.168.1.51 | 00 : 01 : 32 |
| 2021-10-22T00:55:36.1334120-07:00 | E2005114600802621660 6B78 | 1 | -75.5 | 865.7 | 192.168.1.51 | 00 : 01 : 32 |

(b)

Figure 25: (a) Tagged workers being recognized by item test software from Impinj. (b) Details of on-site workers being displayed on a developed web application.

(a)

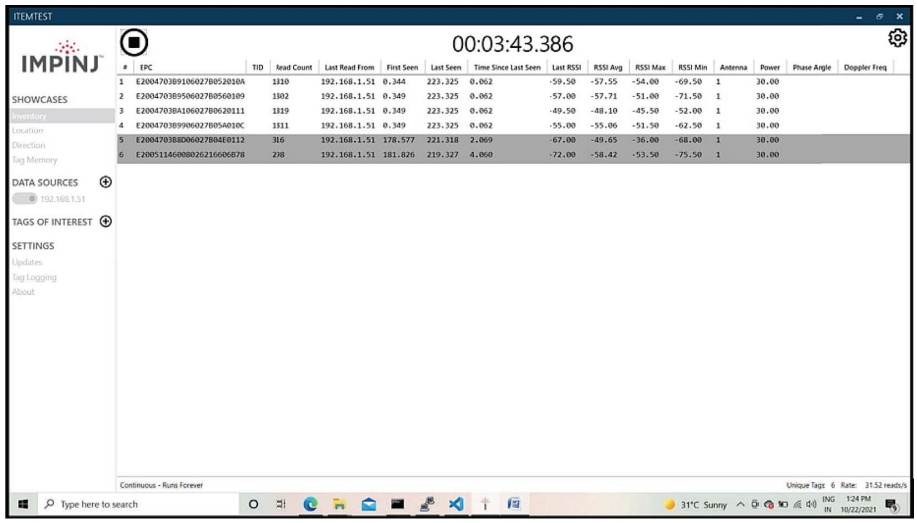


(b)

Onsite Working Details

| // Timestamp | EPC | Antenna | RSSI | Frequency | Hostname | Time Worked |
|---|---|---|---|---|---|---|
| 2021-10-22T00:57:24.3833390-07:00 | E20047i3B9906027B05A010C | 1 | -54 | 865.7 | 192.168.1.51 | 00 : 02 : 19 |
| 2021-10-22T00:57:24.3850790-07:00 | E2004703BA106027B0620111 | 1 | -48 | 865.7 | 192.168.1.51 | 00 : 02 : 19 |
| 2021-10-22T00:57:24.3864460-07:00 | E2004703B9106027B052010A | 1 | -57 | 865.7 | 192.168.1.51 | 00 : 02 : 19 |
| 2021-10-22T00:57:24.3879220-07:00 | E2004703B9506027B0560109 | 1 | -56.5 | 865.7 | 192.168.1.51 | 00 : 02 : 19 |

(c)

FIGURE 26: (a) Construction site with remaining workers (wearing tagged helmets) after few workers left the site. (b) Remaining tagged workers being recognized by item test software from Impinj. (c) Details of on-site workers being displayed on developed web-based application.

the proposed tag antenna is a potential candidate to provide tracking solutions for the workers at complex job sites and, thus, for IoT applications.

## 5. Conclusion

In this work, a standalone RFID system is designed in which an RFID tag antenna equipped with WTMiddleware is developed to provide real-time tracking access control solutions for the workers at risky job sites. For this, a novel tag antenna design with good performance on metallic objects and ABS-based safety helmet is presented. Here, the microstrip patch-based folded dipole configuration is adopted for the tag antenna to exhibit conjugate impedance with respect to the Alien Higgs-3 RFID chip. Here, the information stored in the tag regarding workers in a real-world scenario was processed and accessed by a web-based application through developed WTMiddleware. Thus, RFID readers, tags, and middleware are combined to form a system for registering the workers and monitoring their on-site working status for providing digital worksite visibility of a real job site scenario. Hence, using the developed "IoT-enabled UHF-RFID system" offers a complete solution for the tracking of the workers and effective access control at the real construction job sites.

## Data Availability

No new data were created or analysed in the study.

## Conflicts of Interest

The authors declare that they have no conflicts of interest.

## Acknowledgments

The first Author, Aarti Bansal, is highly thankful to the Department of Science and Technology (DST), Government

of India, for financially supporting the research work under the women scientist scheme (WOS-A) vide reference no. SR/WOS-A/ET-78/2018.

## References

[1] M. Sole, C. Musu, F. Boi, D. Giusto, and V. Popescu, "RFID Sensor Network for Workplace Safety Management," in *Proceedings of the IEEE 18th Conference on Emerging Technologies and Factory Automation (ETFA)*, pp. 1–4, Cagliari, Italy, September 2013.

[2] W. W. S. Chung, S. Tariq, S. R. Mohandes, and T. Zayed, "IoT-based application for construction site safety monitoring," *International Journal of Construction Management*, vol. 23, pp. 58–74, 2020.

[3] G. Alfian, M. Syafrudin, U. Farooq et al., "Improving efficiency of RFID-based traceability system for perishable food by utilizing IoT sensors and machine learning model," *Food Control*, vol. 110, Article ID 107016, 2020.

[4] Y. Ren and H. Li, "Building materials management system based on RFID technology," *International Journal of Reality Therapy*, vol. 9, no. 1-2, pp. 63–74, 2018.

[5] A. Sharif, R. Kumar, J. Ouyang et al., "Making assembly line in supply chain robust and secure using UHF RFID," *Scientific Reports*, vol. 11, no. 1, Article ID 18041, 2021.

[6] M. Gareis, A. Parr, J. Trabert, T. Mehner, M. Vossiek, and C. Carlowitz, "Stocktaking robots, automatic inventory, and 3D product maps: the smart warehouse enabled by UHF-RFID synthetic aperture localization techniques," *IEEE Microwave Magazine*, vol. 22, no. 3, pp. 57–68, 2021.

[7] X. Jia, Q. Feng, T. Fan, and Q. Lei, "RFID technology and its applications in Internet of Things (IoT). 2nd international conference on consumer electronics, communications and networks (CECNet)," *Yichang*, vol. 21-23, pp. 1282–1285, 2012.

[8] G. Li, Z. Li, D. Guan et al., "A hydrogen concentration monitoring system with passive tags," *IEEE Internet of Things Journal*, vol. 8, no. 11, pp. 9244–9256, 2021.

[9] J. Zhang, G. Tian, A. Marindra, A. Sunny, and A. Zhao, "A review of passive RFID tag antenna-based sensors and systems for structural health monitoring applications," *Sensors*, vol. 17, no. 2, p. 265, 2017.

[10] D. Inserra, W. Hu, Z. Li et al., "Screw relaxing detection with UHF RFID tag," *IEEE Access*, vol. 8, pp. 78553–78564, 2020.

[11] Y. Zhang, S. Chen, Y. Zhou, Y. Fang, and C. Qian, "Monitoring bodily oscillation with RFID tags," *IEEE Internet of Things Journal*, vol. 6, no. 2, pp. 3840–3854, 2019.

[12] A. Sharif, J. Ouyang, F. Yang et al., "Low-cost inkjet-printed UHF RFID tag-based system for Internet of Things applications using characteristic modes," *IEEE Internet of Things Journal*, vol. 6, no. 2, pp. 3962–3975, 2019.

[13] X. Wang, J. Zhang, Z. Yu, S. Mao, S. C. G. Periaswamy, and J. Patton, "On remote temperature sensing using commercial UHF RFID tags," *IEEE Internet of Things Journal*, vol. 6, pp. 10715–10727, 2019.

[14] M. Koohestani and A. Ghaneizadeh, "An ultra-thin double-functional metasurface patch antenna for UHF RFID applications," *Scientific Reports*, vol. 11, no. 1, p. 857, 2021.

[15] S. Bauk, "ICT sustavi za poboljšanje sigurnosti na radu u okviru morskih luka," *NAŠE MORE*, vol. 65, no. 2, pp. 94–102, 2018.

[16] D. M. Dobkin and S. M. Weigand, "Environmental effects on RFID tag antennas," in *Proceedings of the IEEE MTT-S International Microwave Symposium Digest*, pp. 135–138, Long Beach, CA, USA, June 2005.

[17] T. Bjorninen, L. Sydanheimo, L. Ukkonen, and Y. Rahmat-Samii, "Advances in antenna designs for UHF RFID tags mountable on conductive items," *IEEE Antennas and Propagation Magazine*, vol. 56, no. 1, pp. 79–103, 2014.

[18] A. A. Babar, T. Bjorninen, V. A. Bhagavati, L. Sydanheimo, P. Kallio, and L. Ukkonen, "Small and flexible metal mountable passive UHF RFID tag on high-dielectric polymer-ceramic composite substrate," *IEEE Antennas and Wireless Propagation Letters*, vol. 11, pp. 1319–1322, 2012.

[19] A. Bansal, S. Sharma, and R. Khanna, "Platform tolerant dual-band UHF-RFID tag antenna with enhanced read range using artificial magnetic conductor structures," *International Journal of RF and Microwave Computer-Aided Engineering*, vol. 30, no. 2, 2020.

[20] E. J. Jaselskis and T. El-Misalami, "Implementing Radio frequency identification in the construction process," *Journal of Construction Engineering and Management*, vol. 129, no. 6, pp. 680–688, 2003.

[21] L. Mo and H. Zhang, "RFID antenna near the surface of metal," in *Proceedings of the 2007 International Symposium on Microwave. Antenna, Propagation and EMC Technologies for Wireless Communications*, pp. 803–806, Hangzhou, China, August 2007.

[22] D. Kim and J. Yeo, "Dual-band long-range passive RFID tag antenna using an AMC ground plane," *IEEE Transactions on Antennas and Propagation*, vol. 60, no. 6, pp. 2620–2626. June, 2012.

[23] D. J. Kern, D. H. Werner, A. Monorchio, L. Lanuzza, and M. J. Wilhelm, "The design synthesis of multiband artificial magnetic conductors using high impedance frequency selective surfaces," *IEEE Transactions on Antennas and Propagation*, vol. 53, no. 1, pp. 8–17, 2005.

[24] I. Y. Park and D. Kim, "Artificial magnetic conductor loaded long-range passive RFID tag antenna mountable on metallic objects," *Electronics Letters*, vol. 50, no. 5, pp. 335-336, 2014.

[25] C. Moh, E. Lim, and B. Chung, "Miniature coplanar-fed folded patch for metal mountable UHF RFID tag," *IEEE Transactions on Antennas and Propagation*, vol. 66, no. 5, pp. 2245–2253, 2018.

[26] Tagfactory, "M-Crown Tag (3-in-1)_95589575.pdf (thetagfactory.com)," 2022, https://www.thetagfactory.com/Admin/downloads/M-Crown%20Tag%20(3-in-1)_95589575.pdf.

[27] Gaorfid, "Small Profile UHF On-Metal RFID Tag (gaorfid.com)," 2022, https://gaorfid.com/product/uhf-on-metal-rfid-tag-6/.

[28] H. Chen, T. K. L. Toh, I. Szeverenyi et al., "Association of skin barrier genes within the PSORS4 locus is enriched in Singaporean Chinese with early-onset psoriasis," *Journal of Investigative Dermatology*, vol. 129, no. 3, pp. 606–614, 2009.

[29] I. Abad, C. Cerrada, J. A. Cerrada, R. Heradio, and E. Valero, "Managing RFID sensors networks with a general purpose RFID middleware," *Sensors*, vol. 12, no. 6, pp. 7719–7737, 2012.

[30] P. Datta and B. Sharma, "A survey on IoT architectures, protocols, security and smart city based applications," in *Proceedings of the 2017 8th International Conference on Computing, Communication and Networking Technologies (ICCCNT)*, pp. 1–5, Delhi, India, July 2017.

[31] S. Bharany, K. Kaur, S. Badotra et al., "Efficient middleware for the portability of paas services consuming applications

among heterogeneous clouds," *Sensors*, vol. 22, no. 13, p. 5013, 2022.

[32] W. Tian, R. Xue, X. Dong, and H. Wang, "An approach to design and implement RFID middleware system over cloud computing," *International Journal of Distributed Sensor Networks*, vol. 9, no. 10, Article ID 980962, 2013.

[33] A. Haibi, K. El Yassini, and K. Oufaska, "Suitcase traceability system via RFID and NoSQL database: middleware, mobile application," *ACM Int. Conf. Proceeding*, vol. 1–6, 2018.

[34] Alien Technology, "Higgs TM 4 IC Datasheet," 2014, http://www.alientechnology.com/wp-content/uploads/Alien-Technology-Higgs-3-ALC-360.pdf.

[35] X. Qing, C. K. Goh, and Z. N. Chen, "Impedance characterization of RFID tag antennas and application in tag Co-design," *IEEE Transactions on Microwave Theory and Techniques*, vol. 57, no. 5, pp. 1268–1274, 2009.

[36] Impinj, 2022, https://supportimpinj.com/hc/en-us/articles/202755388-Impinj-Speedway-RAIN-RFID-Reader-Family-Product-Brief-Datasheet.

[37] S. Bhaskar and A. K. Singh, "A dual band dual antenna with read range enhancement for UHF RFID tags," *International Journal of RF and Microwave Computer-Aided Engineering*, vol. 29, no. 7, pp. e21717–e21718, 2019.

[38] Y. J. Zhang, D. Wang, and M. S. Tong, "An adjustable quarter-wavelength meandered dipole antenna with slotted ground for metallically and airily mounted RFID tag," *IEEE Transactions on Antennas and Propagation*, vol. 65, no. 6, pp. 2890–2898, 2017.

[39] H. Li, J. Zhu, and Y. Yu, "Compact single-layer RFID tag antenna tolerant to background materials," *IEEE Access*, vol. 5, pp. 21070–21079, 2017.

[40] Y. Lin, M. Chang, H. Chen, and B. Lai, "Gain enhancement of ground radiation antenna for RFID tag mounted on metallic plane," *IEEE Transactions on Antennas and Propagation*, vol. 64, no. 4, pp. 1193–1200, 2016.

[41] W. Ng, E. Lim, and B. Chung, "Folded patch antenna with tunable inductive slots and stubs for UHF tag design," *IEEE Transactions on Antennas and Propagation*, vol. 66, no. 6, pp. 2799–2806, 2018.

[42] A. F. M. Fazilah, M. Jusoh, A. Zakaria et al., "Design of compact UHF-RFID tag antenna with meander line technique," *IOP Conference Series: Materials Science and Engineering*, vol. 767, no. 1, Article ID 012058, 2020.

[43] P. Kamalvand, G. Kumar Pandey, M. Kumar Meshram, and A. Mallahzadeh, "A single-sided dual-antenna structure for UHF RFID tag applications," *International Journal of RF and Microwave Computer-Aided Engineering*, vol. 25, no. 7, pp. 619–628, 2015.

[44] P. Kamalvand, G. K. Pandey, and M. K. Meshram, "A single-sided meandered-dual-antenna structure for UHF RFID tags," *International Journal of Microwave and Wireless Technologies*, vol. 9, no. 7, pp. 1419–1426, 2017.

[45] S.-R. Lee, E.-H. Lim, and S. K. A. Rahim, "Small wideband antenna for on-metal UHF RFID tag design," *IEEE J. Radio Freq. Identif.*vol. 6, pp. 121–127, 2022.

[46] M.-T. Nguyen, Y.-F. Lin, C.-H. Chen, Y.-C. Tseng, and H.-M. Chen, "Miniature 3D-dipole antenna for UHF RFID tag mounted on conductive materials," *IEEE Transactions on Antennas and Propagation*, vol. 70, no. 12, pp. 11454–11464, 2022.

[47] F. Erman, S. Koziel, E. Hanafi, R. Soboh, and S. Szczepanski, "Miniaturized metal-mountable U-shaped inductive-coupling-fed UHF RFID tag antenna with defected microstrip surface," *IEEE Access*, vol. 10, pp. 47301–47308, May 2022.